

A NON-CONTACT MONITORING SYSTEM FOR INVESTIGATING AS-BUILT MEMBRANE ROOF STRUCTURES

Shih-Yuan Lin *, Jon P. Mills

School of Civil Engineering and Geosciences, University of Newcastle, Newcastle upon Tyne, NE1 7RU, U.K. –
(shih-yuan.lin, j.p.mills)ncl.ac.uk

KEY WORDS: Monitoring, Dynamic, Video, Surface, Laser Scanning, Matching, Modelling, Engineering

ABSTRACT:

A monitoring system that uses applied geomatics techniques, including terrestrial laser scanning and videogrammetry, has been developed in order to determine the behaviour of as-built membrane roof structures. To accommodate the constraints involved in measuring such structures, for example uniform surface texture and unreachable height, the system adopts a non-contact targeting methodology to substitute for traditional control techniques. This paper reports on experiments conducted to prove that the monitoring system is capable of satisfactorily measuring a typical membrane roof structure. Firstly, in the scheme of investigating the discrepancy between the original design for the membrane roof and the finished version, terrestrial laser scanning is used to produce an as-built model of the membrane structure. The as-built model is then statistically compared with the designed mathematical model using a surface matching approach. The results revealed significant differences between the finished structure and the designed model. Secondly, a sequential 3D surface model was generated from a videogrammetric monitoring scheme, thereby allowing the displacement of the observed area of the membrane surface to be investigated over time. The information acquired from the system is proving to be of great value to structural engineers involved in designing such membrane structures.

1. INTRODUCTION

Since the first membrane roof structure was designed in 1973, their number has increased significantly worldwide due, amongst other factors, to fast construction speeds with extremely competitive unit costs and the fact that such structures provide good durability with low maintenance (Bridgens, 2003). While the characteristics of the material used make various forms and flexible shapes of membrane roof structure possible, a number of engineering problems exist. As a membrane roof resists applied loads, such as that from wind or snow, by a combination of its curvature and tension, it is important to calculate the strength and displacement which are required to withstand the applied forces. Once the structure is built, collapse may occur if the real curvature and tension exceeds the tolerances of the original design. In January 1999, for example, the new membrane roof over Montreal's Olympic Stadium failed, the cause of failure identified as a design fault, not an accident (Parker, 1999a; 1999b). In order to avoid such failures, further research into realising the surface geometry and dynamic behaviour of existing membrane structures is necessary, and is the motivation behind this research.

When considering the development of a membrane roof monitoring system there are two fundamental issues that structural engineers engaged in designing such structures require the scheme to address. The first issue relates to any differences that exist between the designed model and the finished structure, and the second to the displacement of the membrane surface under loading. The overall aim of this project is to develop a generic monitoring system capable of inspecting all manner of membrane roof structures. The geomatics technologies of terrestrial laser scanning and videogrammetry, which are both capable of obtaining real-world 3D models of objects, are introduced in the monitoring system.

Due to the constraints of the working environment (for example, the height of typical membrane roofs), some traditional tasks in videogrammetry are impractical (e.g. targeting for provision of videogrammetric control). Non-contact geomatics techniques are therefore proposed. Having proved to work well under laboratory conditions, the developed monitoring system was deployed to a real-world site (Dalton Park, a retail outlet centre in the north east of England, Figure 1), to verify its feasibility.



Figure 1. Test site – Dalton Park retail outlet centre, U.K.

This paper reports the methodology adopted in developing the monitoring system. In addition the findings of the fieldwork, including the static and dynamic characteristics of the observed membrane structure, will be analyzed and presented in subsequent sections.

* Corresponding author.

2. COMPARISON OF THE MATHEMATICAL AND AS-BUILT MODELS

2.1 Mathematical Design

To understand if any differences were introduced into the roof between the original design drawing and the finished structure, two kinds of models are investigated and compared. The first one is the mathematical model, which is drawn by a structural engineer in the design stage. All the details of the structure, including the supporting steelwork and the membrane surface, are enclosed in the drawing file (Figure 2).

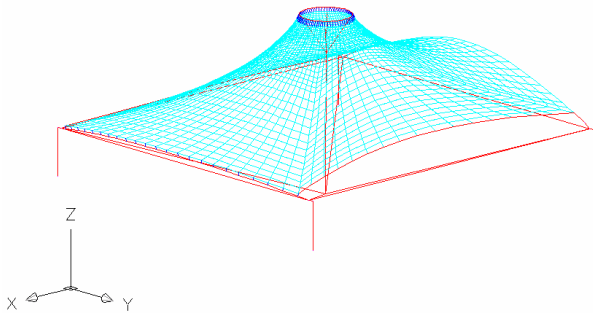


Figure 2. Mathematical model of the membrane roof structure.

2.2 Terrestrial Laser Scanning (TLS)

The second model is derived by applying terrestrial laser scanning, which allows the rapid collection of millions of precisely sampled 3D points of the object (Gordon et al., 2001), forming the basis of a 3D model. In this project a Leica HDS 2500 terrestrial laser scanner was used to acquire the as-built model of the membrane structure. The scanner, with a quoted single-point accuracy of ± 6 mm, gives a 40° by 40° field of view in the horizontal and vertical directions. To completely cover the membrane surface being tested, it was necessary to scan the roof from five scanner stations beneath the structure.

Under normal terrestrial laser scanning procedures, reflective targets are usually arranged in the field of view to permit the combination of each scanned model and registration to a particular reference system. As the height of the structure made the attachment of reflective targets both difficult and inefficient, for model registration some natural detail features on the shop façades beneath the roof were selected as control points instead of attached targets. The polar method was then applied to measure their three dimensional coordinates using a Leica TCRA1103 total station (quoted angular precision of $3''$ and range precision $2\text{mm}+2\text{ppm}$). The resultant registered model of the membrane structure is shown in Figure 3. The amalgamated model has a registration error of 6 mm.

2.3 Surface Matching

Once the mathematical model and the laser scanned model of the membrane structure were available, a surface matching algorithm was used to inspect the differences between the two models. The general problem solved by surface matching relates to finding the optimal rotation and translation parameters that aligns or registers the two point sets or surfaces, one of which may be in an object space coordinate system and the other of which may be in a model coordinate system (Besl and McKay, 1992). By far the most common algorithms used in surface matching have been based on some form of a least squares

adjustment, minimising the differences between the surfaces. Once the matching is finished one of the by-products is the ability to detect changes, as the residuals from the least squares calculation are the surface separations. Examination of these may reveal actual differences that may have occurred between temporal surfaces. Therefore surface matching is an ideal method to be applied in the type of monitoring system described.

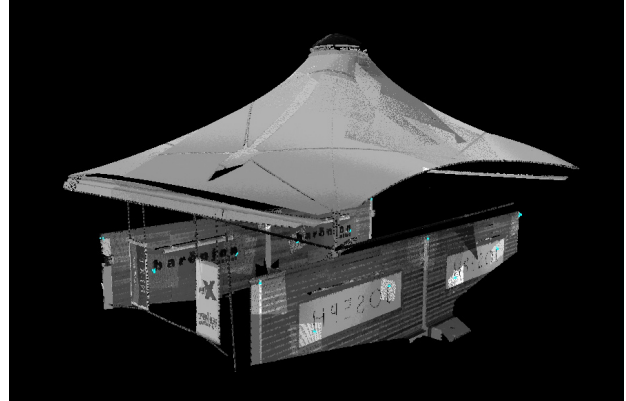


Figure 3. Laser scanned model of the membrane structure.

Identical parts of the membrane surface were extracted from both the laser scanned model and mathematical model. They were then input into 3D Surf (Mills et al., 2005), an in-house surface matching algorithm ideally suited to solving this correspondence problem that was freely available for developmental use in this project. The laser scanned model was deemed as the true model of the membrane surface and was thus input as the reference surface, and the mathematical model was matched to this scanned model. After an initial approximate transformation, the computation of least squares minimisation of vertical differences between the two surfaces was carried out. The solution was iterated until convergence, and the final transformation parameters, as well as the residuals which represented the surface separations, were calculated.

2.4 Surface Model Comparison

To make the matching more efficient, a coarse transformation of the mathematical model to the laser scanned model was implemented before being processed in 3D Surf. The four corners of the two membrane surfaces were selected as common points to compute parameters (Table 1), and the original mathematical model was transformed accordingly. As there should be no change in scale, the scale factor should be fixed to unity. However, the units in the mathematical model were millimetres but metres in the terrestrial laser scanned model. The scale factor was therefore set as 0.001.

Translation (m)			Rotation ($^\circ$)		
T_x	T_y	T_z	ω	ϕ	κ
107.614	61.153	-84.705	0.160	0.147	91.553

Table 1. Parameters for transformation before running 3D Surf.

The transformed mathematical model and laser scanned model were then input into 3D Surf. Once convergence was reached, a total of 12 666 points, evenly distributed across the surface, were used to calculate the residuals. The parameters and residual statistics are listed in Table 2.

Translations (m)	T_x	1.008 ± 0.039
	T_y	-1.891 ± 0.035
	T_z	0.234 ± 0.068
Rotations (°)	ω	-0.525 ± 0.023
	ϕ	-0.109 ± 0.029
	κ	0.485 ± 0.019
Residuals (m)	Maximum	0.305
	Minimum	-0.327
	Range	0.632
	Mean	-0.000
	Std. deviation	0.146
	RMS	0.146

Table 2. Solution from surface matching.

For further analysis of the resolved vertical difference between the two surfaces, the points used for calculating the surface transformation in 3D surf were plotted in their correct planimetric positions; moreover, these points were classified into 10 levels according to the discrepancy values and colour-coded. As shown in Figure 4, the points with a negative value indicated the positions in which the transformed mathematical model was higher than the laser scanned model, and the points with a positive value presented the positions where the transformed mathematical model was lower than the laser scanned model. From the rendered colour it was obvious that the discrepancies occurred symmetrically over the observed surface. Positions (a) to (g) marked in Figure 4 are areas with apparent differences. (a), (c), (d) and (g) were parts the TLS model that were lower than the transformed mathematical model, while (b), (e) and (f) were above.

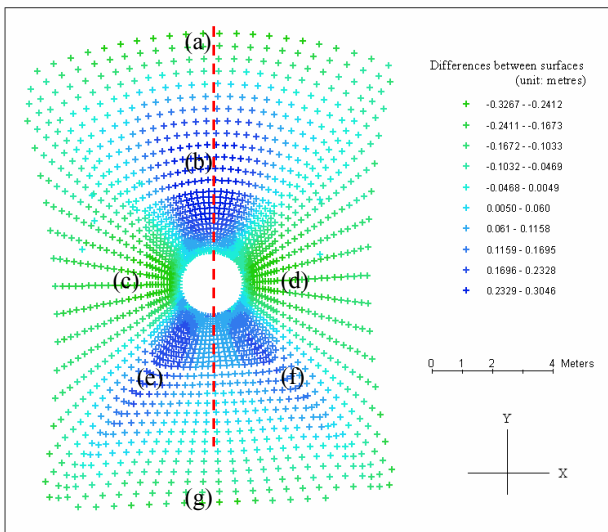


Figure 4. Discrepancies between the two surface models.

Perspective visualisation is another means to view the disparities between the two surfaces. ArcMap and GLView software were employed to create and display the perspective scenes of the matched results. Firstly the mathematical surface model was transformed using the final parameters and then both surfaces were input into ArcMap for meshed model generating and editing. The TLS meshed surface and the matched mathematical model could then be displayed in ArcMap and GLView. Examples of the perspective scene shown in GLView are illustrated in Figure 5, and the areas of obvious difference specified in Figure 4 are pointed out in the 3D surface model.

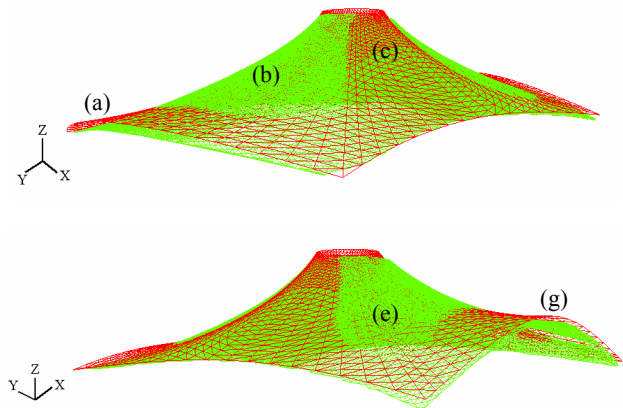


Figure 5. Resultant meshed models after surface matching (green mesh: laser scanned model; red mesh: transformed mathematical model).

In addition, profile comparisons and corresponding metric information were queried using in-house software. The difference value and the shape of the specific part of the membrane surface could be investigated through the extracted profiles. Take Figure 6 for example, the diagrams shown herein display the profile along the dashed line in Figure 4. The green profile line was derived from the laser scanned model, and the red line represented the profile of the transformed mathematical model. The blue curve shown in the figure below illustrates the difference values between the two profiles. Along the profile the discrepancies occurred in areas (a), (b) and (g) were inspected; also, the disparity in the top middle part of the membrane surface was determined.

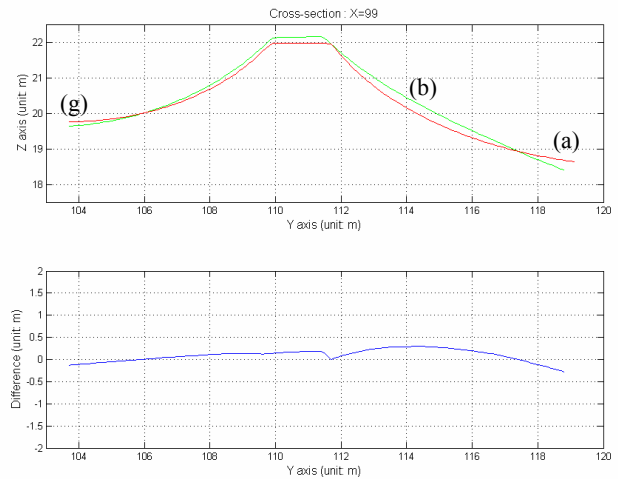


Figure 6. Differences in profile between the two surface models.

Based on the metric information and the model visualisation presented above, it is shown that significant differences exist between the finished “as-built” membrane roof structure and the designed mathematical model. This situation is suspected to result from an error that occurred during structure construction in which the middle flying mast was propped higher than designed, while the front curved beam, area (a), was lower than the designed height, deforming the membrane surface in area (b). As yet this is the preliminary inference, and further investigations are being conducted.

3. DYNAMIC BEHAVIOUR OF THE MEMBRANE SURFACE

3.1 Videogrammetry

Videogrammetry is the science of calculating 3D object coordinates as a function of time from image sequences captured by video cameras. It expands the method of photogrammetry to multiple time steps, enabling the observed object to be defined dynamically (Black and Pappa, 2003). Although photogrammetry is not restricted to static or non-dynamic applications (e.g. Maas et al., 2003; Ryall and Fraser, 2002), videogrammetry has been used in moving object measurement and trajectory tracking and has therefore been adopted in this project for monitoring the dynamic behaviour of membrane roof surfaces.

Three consumer-grade digital video (DV) camcorders, JVC GR-D30U, Sony DCR-PC101 and Sharp VL-Z1, capable of capturing image sequences were employed in this project. Their portable size and the internal LCD monitor allowed handy adjustment of camera stations and on-site quality assurance of the acquired imagery. The recorded imagery could be directly downloaded to the host computer via IEEE1394 (Firewire) interface. These DV camcorders are all manufactured to meet National Television Standards Committee (NTSC) TV standard, which defines the sampling rate as 29.97 frames per second and the image resolution of a single frame grabbed from a video image sequence as 720 pixels by 480 pixels (PCTechGuide, 2003). Their low cost, potentially enabling the deployment of multiple systems in the event that the research is ultimately successful, and ease of use by on-site engineers made them particularly attractive for this research.

During the task of constructing a surface model by videogrammetry, it is common to use some form of targeting for videogrammetric network control, and there is also a requirement to synchronise contemporary image frames from the different cameras used. Moreover, in order to determine a surface model, the targets for measurement should ideally be located extensively across the surface. However, due to the constraints involved in measuring such a structure, e.g. the uniform surface texture and unreachable height, traditional methods of targeting are generally not practicable. To solve these problems, alternative methods of providing control and targets were adopted in this project.

3.2 Non-Contact Control Methodology

A certain number of control points in object space are generally required for videogrammetry applications. Object space coordinates of control points, which must be image-identifiable features, are normally determined in traditional close range photogrammetry via some type of field survey, usually utilising a total station. However, in this case it is difficult to identify reliable features on the object or to attach physical targets to act as control points. To accommodate this particular situation, a laser scanning or reflectorless EDM technique offers an alternative solution whereby visible laser footprints are imaged by the DV cameras being used. Because the footprints are visible in the acquired video images and have associated 3D coordinates, they have the potential to be used as control points. Furthermore, they can also be used to synchronise simultaneous image frames captured from different cameras. Lin and Mills (2005) have proved the idea is applicable, demonstrating comparable performance to conventional control methods.

In this project a motorised total station (Leica TCRA1103, featuring a reflectorless EDM with visible laser) was used to generate the laser footprint control. Once the total station was setup, an in-built scanning program was executed and a sequence of points was automatically measured directly on the surface of the membrane structure. Meanwhile the three DV camcorders, calibrated using the PhotoModeler Calibration Module (a procedure that was independently verified), were arranged in the most appropriate network configuration given workplace and other constraints (Fraser, 2001) and triggered to acquire image sequences of the laser footprints. These laser footprints, complete with 3D coordinates, were recorded in different frames of the acquired image sequences. Appropriate image frames were identified and combined using an image arithmetic algorithm to produce a control image for each exposure station (Figure 7). The image coordinates of the laser footprints were then introduced into the videogrammetric process as control points.

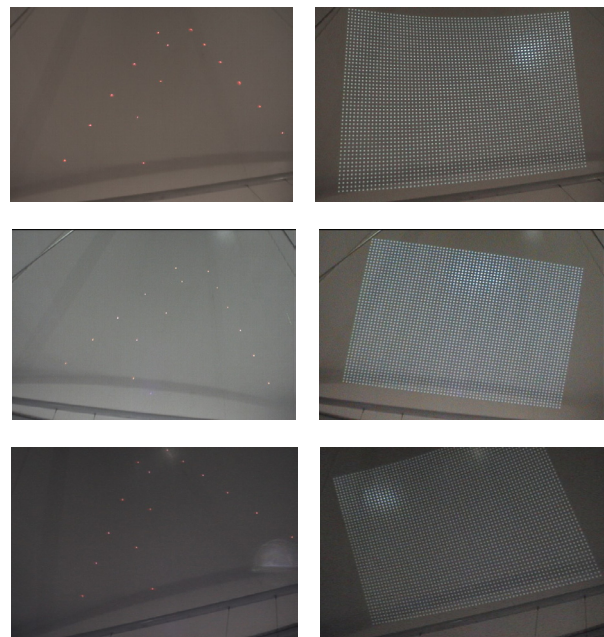


Figure 7. Images of control points (left) and example frames of projected targets (right).

3.3 Projected-dot Videogrammetry

A complete and accurate surface model will be determined from videogrammetry if there are sufficient artificial targets or natural features on the surface to measure. However, as the membrane surface lacks identifiable texture and its height makes attaching targets difficult, physically attached targets were substituted with projected light dots. The use of projected dots as targets is not only time-effective, but also allows customization to any density or size, providing greater flexibility than attached targets (Ganci and Brown, 2000). For long-term dynamic surface monitoring, an appropriate design of dot pattern is continually projected onto the surface of interest and the changes in position of the projected dots over time are recorded by the DV camcorders. Figure 7 illustrates simultaneous frames of projected-dots grabbed from the three image sequences. Data capture took place at night due to the use of a relatively low powered projector, although this limitation could potentially be overcome by using a projector with a brighter lamp.

Once the monitoring was complete, the image sequences were downloaded to the host computer. Before surface extraction could take place, image pre-processing tasks such as image enhancement, segmentation and synchronisation were conducted using in-house software, programmed using the MATLAB language. Projected targets were then extracted from the image frames and the measured points were matched to corresponding targets taken from other exposure stations.

PhotoModeler software was used to perform a bundle adjustment, necessary for solving the 3D positions of the projected targets. To accomplish this, all information obtained from the previous stage was input into PhotoModeler. Dynamic Data Exchange (DDE) technology, which facilitates communication of two Windows applications, was introduced to extend the level of automation (Eos System Inc., 2004; The MathWorks, Inc., 2004). The DDE conversation was established to access PhotoModeler through MATLAB code, therefore the tasks (including data import, bundle adjustment implementation, solution export, etc.) could be triggered in MATLAB, rendering the manual operations in PhotoModeler entirely unnecessary and thereby improving the performance of the monitoring system. Once the bundle adjustment reached convergence, the results were exported to MATLAB for further analysis. In each temporal epoch, the 3D positions of 2300 points were computed with a measurement precision of +/- 7 mm (Figure 8). The surface model was subsequently produced by interpolation of the estimated points and the dynamic model of the membrane surface was determined from the computed 3D surface model at various epochs (Figure 9).

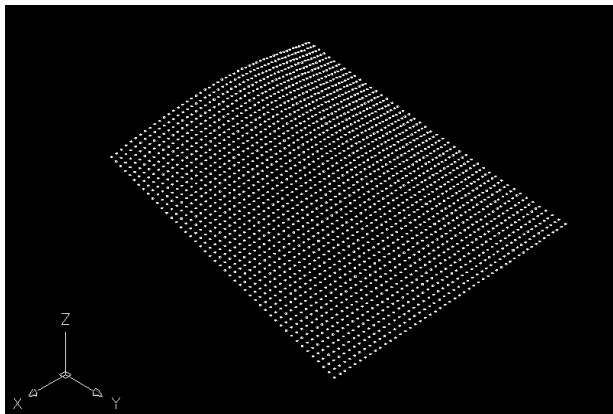


Figure 8. Point model generated at the first temporal epoch.

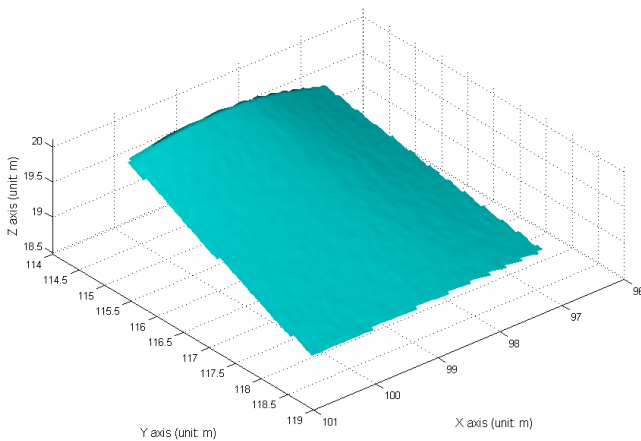


Figure 9. Surface model generated at the first temporal epoch.

The relatively poor measurement precision was attributed to the low resolution and specification of the DV camcorders used (object space pixel sizes varied between 9 mm and 11 mm). Therefore, digital video cameras featuring higher image resolution, two eight-megapixel Oscar OF-810C cameras, were tested as alternatives in the monitoring system. Due to the variability of the image formats and scan modes, users can select a suitable setting of the video cameras for specific applications. In preliminary experiments two cameras with 1088 pixels by 822 pixels format and progressive scan mode were adopted, and the measurement precision was determined as +/- 1.3 mm. Due to the improved performance, the Oscar cameras will be introduced in future fieldwork, but further results are not reported in this paper.

3.4 Sequential Displacement

Displacement that occurred between any two epochs (nominal one second interval in this experiment) can be queried using the developed software. One of the outputs is statistical information, for example Table 3 lists the displacements determined between epochs 1 and 2. External wind loading was considered to be the main cause of expected displacement, but as weather conditions were very good on the day the experiment was conducted, little movement was anticipated and indeed the displacements observed in the sequential surface model were largely insignificant. It is anticipated that the introduction of the Oscar cameras (Section 3.3) will improve the sensitivity of the system.

Displacement (m)	Maximum	0.016
	Minimum	-0.015
	Range	0.031
	Mean	-0.001
	Std. deviation	0.004
	RMS	0.004

Table 3. Displacement statistics between epochs 1 and 2.

In addition to the statistics, a displacement map is also produced. For further visualisation, diagrams are created that show the differences of Z-ordinates between any two meshed models. By viewing the map of displacement between epoch 1 and 2 (Figure 10), the positions of the differences could be realised.

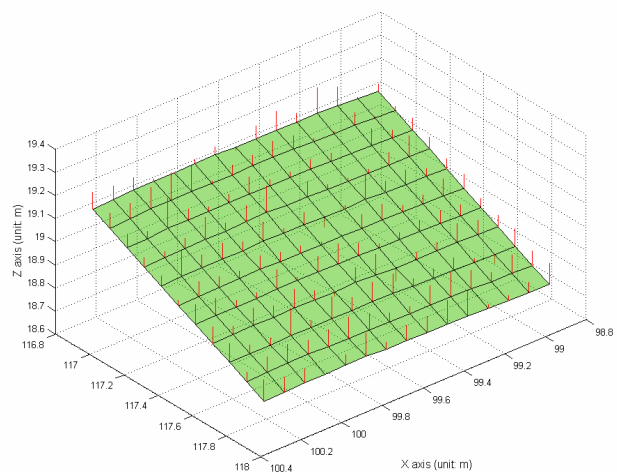


Figure 10. Close-up view of the displacement of the observed surface. The base is the surface model of the 1st epoch, the vectors (which is ten times magnified) represent the differences to the 2nd epoch.

4. COMBINATION OF SURFACE MODELS

Finally, as the videogrammetric and the laser scanned models are constructed under the same coordinate system, the models can be combined together. This enables visualisation of the exact area of the membrane roof onto which the targets were projected (Figure 11).

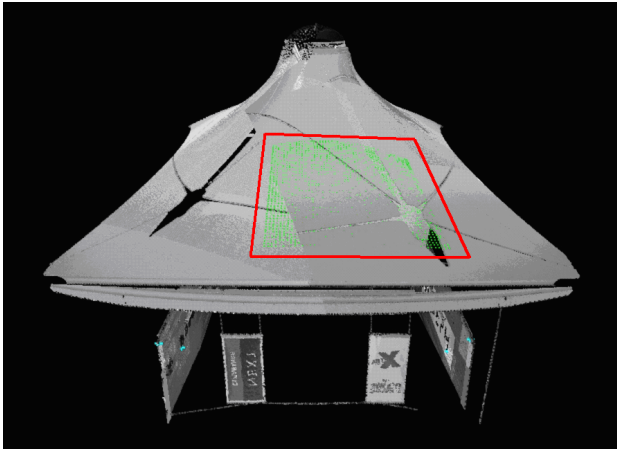


Figure 11. Laser scanned (monochrome) and videogrammetric (green points outlined by red line) models.

5. SUMMARY AND FUTURE WORK

To realise the static and dynamic behaviour of membrane roof structures, a monitoring system that applies terrestrial laser scanning and videogrammetry has been developed. It has been proven capable of measuring an as-built membrane structure. Firstly, the as-built membrane structure was modelled through terrestrial laser scanning. Surface matching methods were used to compare the original designed mathematical model and the laser scanned model, and the discrepancies between them were identified. Overall analysis revealed significant differences between the finished structure and the designed model.

Secondly, in the videogrammetric task, the proposed non-contact targeting method is accommodated to the constraints in the working environment. By analysing a sequence of surface models, displacement and deformation of the structure can be determined over time. The information acquired by the system is proving to be of great value to collaborating engineers who are involved in designing such membrane structures.

In future research, a more robust membrane structure monitoring system will be developed. This will include the use of higher resolution digital video cameras to improve measurement precision, extended automation and an improved user interface for the monitoring system. Further testing will be conducted under heavier loading conditions and transferability will be assessed by applying the system to different types of membrane structure.

ACKNOWLEDGEMENTS

The authors would like to thank Dr. Peter Gosling, Reader in Computational Structural Mechanics at the University of Newcastle upon Tyne, and Arup for providing the mathematical model of the Dalton Park membrane structure.

REFERENCES

- Besl, P. J. and McKay, N. D., 1992. A method for registration of 3-D shapes. *IEEE transactions on Pattern Analysis and Machine Intelligence*, 14(2): 239-256.
- Black, J. T. and Pappa, R. S., 2003. Videogrammetry using projected circular targets: proof-of-concept test. <http://techreports.larc.nasa.gov/ltrs/PDF/2003/tm/NASA-2003-tm212148.pdf> (accessed 21st November 2003).
- Bridgens, B. N., 2003. Non-linear material models for coated woven fabrics. <http://hometown.aol.com/bridgensb/Fabrics.htm> (accessed 23rd September 2003).
- Eos Systems Inc., 2004. *PhotoModeler Pro 5 User Manual*, Vancouver B. C., Canada. 500 pages: 397-419.
- Fraser, C. S., 2001. Network design. *Close range Photogrammetry and Machine Vision* (Ed. K. B. Atkinson). Whittles Publishing, Caithness. 371 pages: 256-281.
- Ganci, G. and Brown, J., 2000. Developments in non-contact measurement using videogrammetry. <http://www.geodetic.com/Downloadfiles/Developments%20in%20Non%20Contact%20Videogrammetry.pdf> (accessed 24th November 2003).
- Gordon, S., Lichti, D. and Stewart, M., 2001. Application of a high-resolution, ground-based laser scanner for deformation measurements. http://rincon.gps.caltech.edu/FIG10sym/pdf/Session%20I_Paper%204.pdf (accessed 14th November 2003).
- Lin, S. Y. and Mills, J. P., 2005. A non-contact method of controlling videogrammetry in surface modelling applications. *Optical 3-D Measurement Techniques VII* (Eds. A. Gruen and H. Kahmen). Vienna, Austria. Volume II: 124-132.
- Maas, H. G., Hentschel, B. and Schreiber, F., 2003. An optical triangulation method for height measurements on water surfaces. *Proceedings of the SPIE Symposium - Electronic Imaging 2003 (Videometrics VIII)*. Santa Clara, California, USA. Volume 5013: pp. 103-109.
- Mills, J. P., Buckley, S. J., Mitchell, H. L., Clarke, P. J. and Edwards, S. J., 2005. A geomatics data integration technique for coastal change monitoring. *Earth Surface Processes and Landforms*, 30(6): 651-664.
- Parker, D., 1999a. Dome supplier faces Montreal compensation battle. *New Civil Engineer*, 28 January: 4.
- Parker, D., 1999b. Are giant tents domed? *New Civil Engineer*, 4 February: 16-19.
- PCTechGuide, 2003. Digital video format. http://www.pctechguide.com/24dvid3.htm#DV_format (accessed 14th December 2003).
- Ryall, T. G. and Fraser, C. S., 2002. Determination of structural modes of vibration using digital photogrammetry. *AIAA Journal of Aircraft*, 39(1): 114-119.
- The MathWorks, Inc., 2004. Dynamic data exchange. *MATLAB 7.0 on-line help documents*.